Geoenvironmental Disasters

RESEARCH

Open Access

Experimental study on the buffering mechanism of EPS bead-sand cushions under single and multiple impacts

Feifan Ren[1,2], Jiahao Liu[3], Qiangqiang Huang[4], Huan Ding[3], Zhipeng Hu[3] and Guan Wang[5*]

Abstract
As a main functional component of rock sheds in rockfall protection projects, traditional sand cushions have shortcomings such as heavy weight and weak buffering capacity. EPS bead-sand cushion can effectively solve these problems, but its buffering mechanism has not been fully revealed. In this study, a series of impact tests were carried out to investigate the performance of EPS bead-sand cushions with different EPS bead contents, and the evolutions of rockfall impact force, penetration depth, earth pressure, and slab vibration under single impact and multiple impacts were comparatively analyzed. The results show that with the addition of EPS beads, the maximum impact force, the peak earth pressure, and the vibration acceleration are significantly reduced. However, the cushion with high EPS bead content is at risk of being penetrated under high energy or multiple impacts, leading to excessive concentration of impact stresses. Furthermore, the EPS beads can alleviate the hardening of the sand cushion under impact through their deformation coordination, but excessive penetration should be prevented in the design of EPS bead-sand cushions. On this basis, combined with traditional sand cushion design theory, an estimation method for the maximum impact force applicable to EPS bead-sand cushion was proposed. The research results can provide a reference for the design and optimization of cushions in actual projects.

Keywords Cushion, EPS beads, Impact force, Earth pressure, Acceleration

*Correspondence:
Guan Wang
wangguan@usst.edu.cn
[1]Key Laboratory of Geotechnical and Underground Engineering of Ministry of Education, Department of Geotechnical Engineering, Tongji University, Shanghai 200092, China
[2]State Key Laboratory of Disaster Reduction in Civil Engineering, College of Civil Engineering, Tongji University, Shanghai 200092, China
[3]Department of Geotechnical Engineering, College of Civil Engineering, Tongji University, Shanghai 200092, China
[4]Department of Geotechnical Engineering, College of Civil Engineering, Tongji University, Shanghai 200092, China
[5]School of Environment and Architecture, University of Shanghai for Science and Technology, Shanghai 200093, China

Introduction

Complex geological environments and engineering disturbances often lead to geological disasters. In 2021, a total of 4,761 geological disasters occurred in China, resulting in 3.2 billion economic losses, of which 1,746 are rockfall geological disasters, accounting for 36.67% of the total number of geological disasters (National Bureau of Statistics of China 2023). Rockfall is a broken rock or block separated from the surface slope or cliff by falling, sliding, tipping, bouncing, or rolling (Wei et al. 2014; Žabota & Kobal 2020), which has the characteristics of large kinetic energy, high frequency of occurrence, strong uncertainty and great harm (Dorren 2003). As a passive protection measure, rock shed has the characteristics of high efficiency, strong interception ability, and simple construction (He et al. 2014; Zhao et al. 2018b; Yu et al. 2019), and the reinforced concrete structure is a commonly used structural form (Liu et al. 2020; Zhao et al. 2021). Placing a cushion on the rock shed is an effective and low-cost method against rockfall (Bhatti, 2014), which can dampen vibration, extend impact duration time, decrease impact force, and dissipate impact energy.

The choice of buffering material is mainly based on local soil, with sand having the best buffering performance, followed by clay, loam, and yellow-brown loam (Luo et al. 2019). It has been shown that as the thickness of the cushion increases, the better the buffering effect is, and the smaller the impact force suffered by the rock shed is. (Kawahara and Muro 2006; Xu 2016; Yao 2018; Shen et al. 2021). However, the load supported by the rock shed will increase as the cushion thickness increases, thereby increasing the construction cost of the rock shed (Yu et al. 2019). On this basis, Expanded polystyrene (EPS) material was introduced to the cushion to decrease the weight and increase the damping ratio and energy consumption (Khajeh et al. 2020), and a new EPS cushion made of steel grille, sand, and EPS board was proposed by Hsu et al. (2016, 2018). It is estimated that a cushion consisting of sand and EPS board can significantly increase the buffering capacity, even the impact force can reach a reduction of 75% by placing the EPS board in the proper position. (Zhao et al. 2018a; Ertugrul and Kiwanuka 2023), and thicker geofoam is favorable to reduce the impact force (Yan et al. 2022; Zhang et al. 2022; Zhao et al. 2023).

Although EPS boards have many advantages, some problems have been exposed with their promotion and use. For instance, EPS boards are difficult to replace and are prone to plastic deformation and damage under the large-energy impact, which significantly reduces their buffering and energy-consuming performance (Zhao et al. 2018a). Furthermore, EPS boards are difficult to transport and have limited application in challenging work environments. On this basis, Ge et al. (2022) introduced an EPS bead layer into the cushion, and the test results showed that the EPS bead layer had a better performance in reducing the impact force. Compared with EPS board, EPS beads offer superior compressive performance, strong durability, ease of replacement, and deformation resilience. It can be extruded from leftover EPS materials and has a porous structure that effectively disperses external stress. Additionally, EPS light soil has been widely used in slope repair, vibration reduction, light backfilling of retaining walls and embankments, and backfilling of concentrated areas of underground facilities (Alaie and Chenari 2018; Alaie and Jamshidi 2019; Khajeh et al. 2021; Alaie et al. 2020; Hou and Yang 2021). Although there are many benefits to using EPS beads as a buffering material, there are currently few studies on EPS beads composite cushions, particularly when EPS beads are mixed with sand, and the performance of the cushion is greatly impacted by the EPS beads content (Deng and Xiao 2010). In addition, with global warming and the frequent occurrence of extreme weather, the cushion often needs to withstand multiple rockfall impacts during its life cycle, and the buffering efficiency of the cushion under multiple impacts is also worth discussing.

In this study, a comparative study on the rockfall impact resistance behavior of EPS bead-sand cushion with different EPS bead contents was conducted through a series of impact tests. The change patterns of rockfall impact force, penetration depth, earth pressure, and slab vibration under single impact and multiple impacts were explored. At the same time, the impact stress factor was introduced to analyze the diffusion and attenuation rules of impact stress in the cushion. On this basis, combined with traditional sand cushion design theory, an estimation method of the maximum impact force of the cushion with different EPS bead contents was proposed. The research results can provide a reference for cushion design and optimization in geological disaster prevention and control projects.

Rockfall impact test

Materials

Sand

A river sand was used as the main buffering material, with a particle size of 0 ~ 5 mm, and the grading curve is shown in Fig. 1. The unevenness coefficient C_u is 3.68 and the curvature coefficient C_c is 1.03, indicating that it is a poorly graded soil.

EPS beads

Spherical EPS beads with a diameter of 2 ~ 4 mm were used in this study, as shown in Fig. 2(a). The density of EPS beads is 0.019 g/cm^3, with the characteristics of uniform particles, good deformation resilience, and long service life.

EPS bead-sand mixture

The buffering material consists of a mixture of sand and EPS beads, and the mass ratios of EPS beads discussed in this study are 0%, 0.25%, 0.5%, and 0.75% respectively. The maximum and minimum dry densities for different EPS bead contents are shown in Table 1, and the relative density was uniformly taken as 50%. Moreover, EPS beads and sand were mixed by mechanical agitation and a 5% mass ratio of water needs to be added to ensure uniform mixing (Fig. 2b) (Alaie and Jamshidi 2019).

In addition, through triaxial testing, the variation curves of the deviatoric stress q with the axial stress ε of the EPS bead-sand mixtures were obtained, as shown in Fig. 3. As the EPS bead content increases, the peak

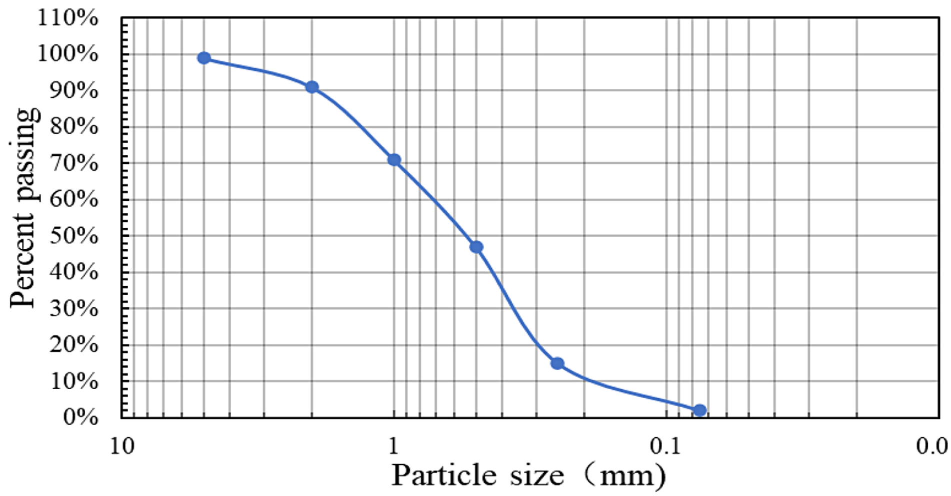

Fig. 1 Sand grading curve

Fig. 2 Buffering materials: (**a**) EPS beads; (**b**) EPS bead-sand mixture

Table 1 Maximum and minimum dry density of the sand with different EPS bead content

EPS beads mass ratio	Maximum dry density(g/cm^3)	Minimum dry density(g/cm^3)	Relative density	Cushion density (g/cm^3)
0.00%	1.95	1.50	50%	1.70
0.25%	1.74	1.23	50%	1.44
0.50%	1.56	1.02	50%	1.23
0.75%	1.40	0.91	50%	1.10

deviatoric stress decreases. It is worth noting that with the increase of EPS bead content, the axial strain at peak shear stress increases. This is because EPS beads absorb some of the shear deformation, resulting in large deformation of the sample to form a shear plane, and the absorption effect becomes more obvious with the increase of EPS bead content. Moreover, When the EPS bead content exceeds 0.5%, there is no obvious peak in deviatoric stress, indicating that the EPS beads have significantly reduced the strength of the mixture, leading to gradual deformation rather than the formation of a distinct shear plane. The internal friction angles of the mixtures with EPS bead content of 0%, 0.25%, 0.50%, and 0.75% were obtained to be 40.1°, 37.1°, 33.6°, and 31.4°, respectively, and the cohesive force was 0 kPa.

Experimental design

Scaling factor considerations

It is very important to correctly scale down prototypes and select appropriate materials during model testing. However, according to the similarity theory, it is difficult to fully meet the similarity conditions of the prototype under the 1 g scaled model, so scaled models are usually designed based on some key variables. Acceleration (A), as a key index, is often regarded as a fundamental quantity for kinetic analysis between models and prototypes

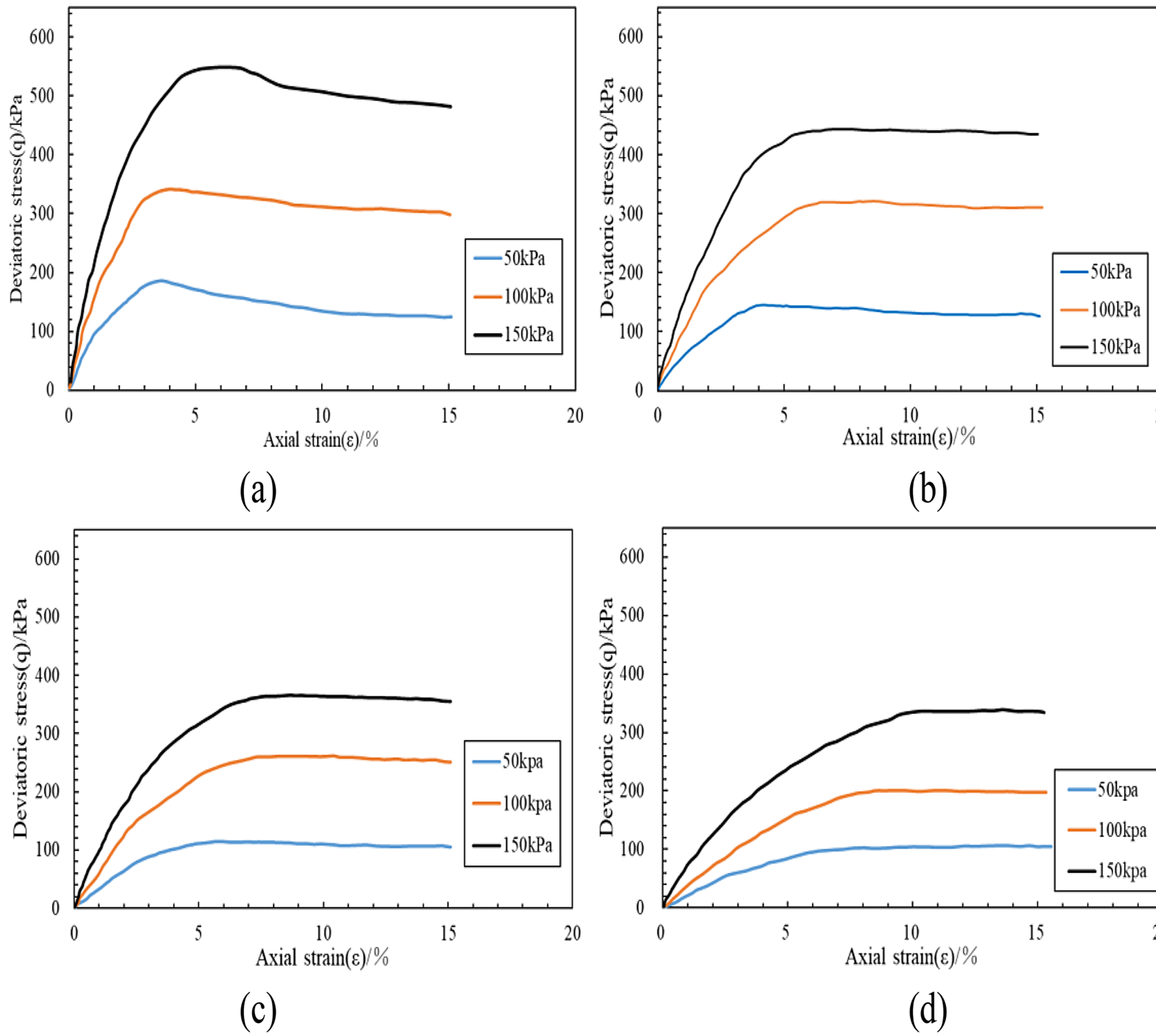

Fig. 3 Deviatoric stress-axial strain curves of EPS bead-sand: (**a**) pure sand; (**b**) 0.25% EPS bead-sand; (**c**) 0.50% EPS bead-sand; (**d**) 0.75% EPS bead-sand

Table 2 Model similarity ratio

Quantity	Similitude relation	prototype	Scaling factor [a]
Geometric dimensions	S_L	1	N^{-1}
Density	S_ρ	1	1
Acceleration	S_a	1	1
Elastic modulus	S_E	1	N^{-1}
Stress	S_σ	1	N^{-1}
Impact force	S_F	1	N^{-3}
Impact energy	S_w	1	N^{-4}
Duration time	S_t	1	$N^{-\frac{1}{2}}$
Poisson's ratio	S_v	1	1

[a] N = scale factor

(Ren et al. 2020; Cai et al. 2021). The density of the buffering material (ρ) is usually consistent with the prototype (Meng et al. 2022), and the geometric dimensions need to be taken into account as well. The related scaling factors are shown in Table 2.

In this study, the scale factor N was taken as 6. Considering the energy dissipation capacity of the cushion and the gravitational force acting on the rock shed, the cushion thickness was taken as 0.15 m in the model with reference to the recommended cushion of 0.9 m thickness in Japanese engineering practice (Meng et al. 2022). Moreover, the weight and height of rockfall in actual projects range from 100 to 10,000 kg and 5 to 50 m, respectively (Di Prisco and Vecchiotti 2010), and the proportion of rockfall events with impact energy less than 100 kJ is 68% (Wang et al. 2016). Therefore, according to Table 2, the

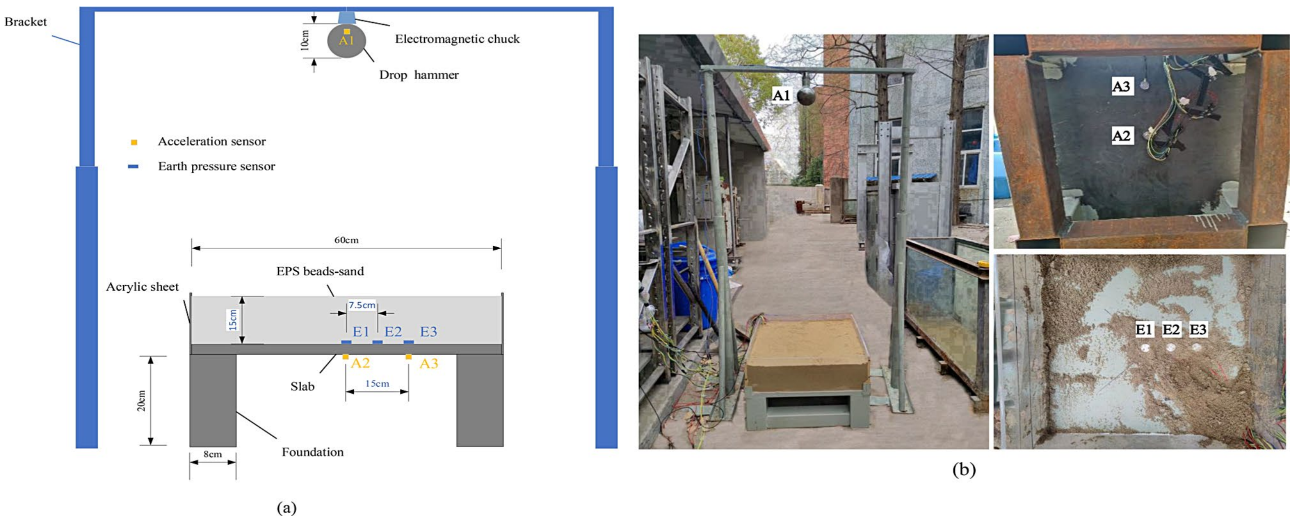

Fig. 4 Sketch of the model test: (**a**) model sketch layout ; (**b**) sensor arrangement

weight and height of rockfalls in the model tests were taken to be 0.5 ~ 46.3 kg and 0.8 ~ 8.3 m, respectively. In addition, since spherical rockfalls are often used in tests (Zhang et al. 2022; Wang et al. 2019), to obtain sufficient impact energy at a limited height, a spherical iron ball with a diameter of 0.1 m and a weight of 4.4 kg was used in this test. At the same time, the cushion width should be at least 6 times the diameter of the iron ball to reduce the influence of boundary conditions, so the cushion width was taken to be 0.6 m. Additionally, a welded steel frame was used to simulate the rock-shed structure, and acrylic plates (0.2 m in height) were used to constrain the buffering material. A retractable bracket was used to control the release height of the falling ball (as shown in Fig. 4), and three situations of 0.7 m, 1.1 m, and 1.5 m were considered for the release height of the falling ball.

Table 3 Model test variables

Model test	EPS beads mass ratio	Impact height(m)	Number of impacts
sand	0%	0.7	4
		1.1	1
		1.5	1
0.25%EPS	0.25%	0.7	4
		1.1	1
		1.5	1
0.5%EPS	0.5%	0.7	4
		1.1	1
		1.5	1
0.75%EPS	0.75%	0.7	4
		1.1	1
		1.5	1

Setup of experiment

The cushion was compacted in three layers by controlling the relative density. Before the test began, the falling ball was absorbed at a specific height (0.7 m, 1.1 m, and 1.5 m) through an electromagnetic chuck. Then the falling ball was released by controlling the electromagnetic chuck, and the falling ball fell freely and impacted the center of the cushion. In the model tests, the impact energies exerted by the falling ball are 30.18 J, 47.43 J, and 64.68 J respectively, corresponding to 39.1 kJ, 61.5 kJ, and 83.8 kJ in the prototype. In addition, an acceleration sensor A1 (range 100 g) was installed inside the falling ball to monitor the impact force acting on the cushion, and acceleration sensors A2 and A3 (range 10 g) were installed at the bottom of the slab to monitor the vibration of the slab. Meanwhile, Earth pressure gauge E1 was installed at the center point of the upper surface of the slab, and E2 and E3 were installed 10 cm apart to monitor the impact stress acting on the slab (Fig. 4b).

The tests were conducted to investigate the performance of the cushion with different EPS bead contents under single impacts with different impact energies and multiple impacts with the same impact energy. Since the 0.7 m release height corresponds to the actual impact energy of 39.1 kJ, which meets the impact energy of rockfall in most cases, the 0.7 m release height was chosen for multiple impacts in this study. There are four groups of working conditions (Table 3), in which each group of working conditions was continuously impacted 4 times at an impact height of 0.7 m, while only impacting once at 1.1 m and 1.5 m heights. It should be noted that after each impact, the cushion was completely removed and the model was rebuilt before proceeding to the next test. To demonstrate the repeatability of the tests and to assess

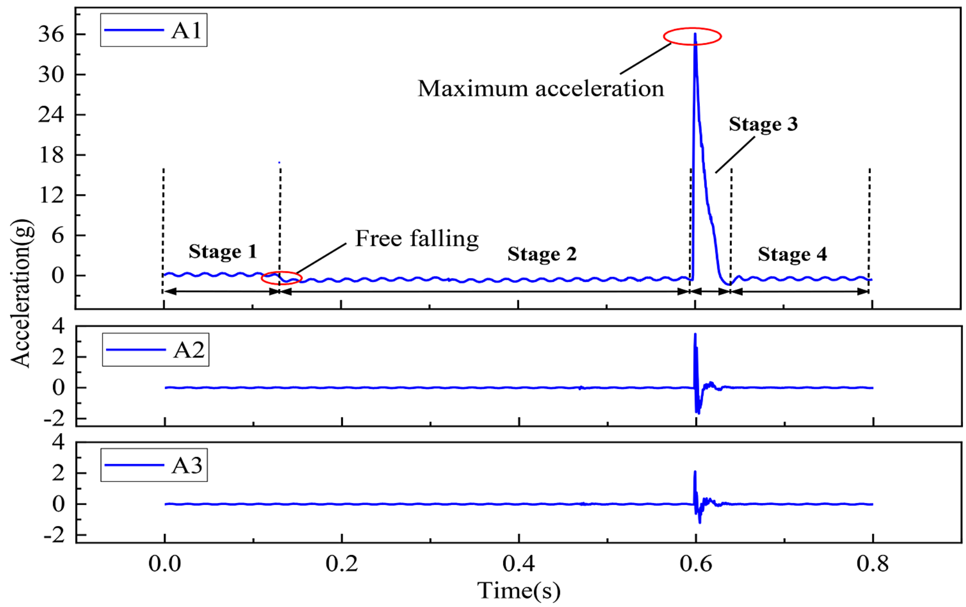

Fig. 5 Time history of acceleration

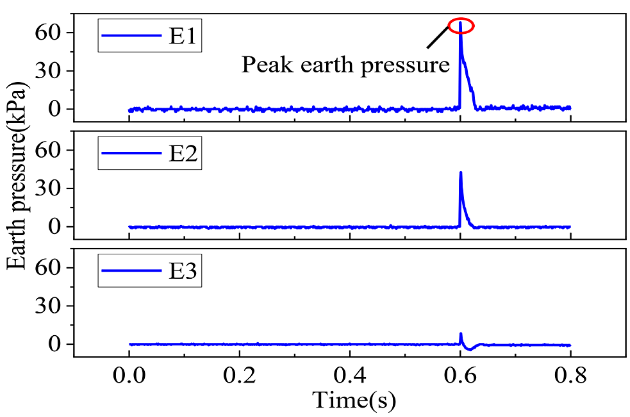

Fig. 6 Time history of earth pressure

the variability of the test results, three replicate tests were conducted for each type of cushion.

Test results

Time histories of acceleration and earth pressure

The impact acceleration, slab vibration acceleration, and earth pressure were measured in this test. Taking the sand cushion with a single impact energy of 47.43 J as an example, the time history curve of impact acceleration (A1) can be divided into four stages, as shown in Fig. 5. In the first stage, the falling ball is stationary, and A1 stays near 0. The falling ball enters the second stage when the electromagnetic chuck is shut off, the acceleration quickly reaches -g. In the third stage, the falling ball impacts the cushion, and the acceleration rapidly increases to the peak value, and then quickly decreases to a minimum value. The impact energy is dissipated in this process. The fourth stage is the dissipation of the remaining impact energy.

During the third stage, the slab vibrated under the impact, and the acceleration responses of A2 and A3 are shown in Fig. 5. The acceleration stayed near 0 before the impact; then Acceleration fluctuated under the impact. As the vibration weakens, the acceleration gradually converges to 0. A2 and A3 have different amplitudes, but the patterns are almost the same. In addition, the earth pressure shows a change pattern consistent with the acceleration, and it is noteworthy that the impact duration of the A1 and E1 is almost equal (Fig. 6), and the peak earth pressure shows as E1 > E2 >> E3. However, instead of going to 0 after peaking, E3 has a minimum value. This is because E3 is far away from the center point of the cushion, and the impact force is distributed in a cone shape (Wang et al. 2018). The buffering material around the center was squeezed under the impact, and E3 was subjected to lateral extrusion, thus generating a negative value.

Depth of penetration

The penetration depth(D_p)of the falling ball is often used to characterize the size of an impact crater. D_p is defined as $\Delta Y/H$, where Y is the actual penetration depth and H is the thickness of the cushion layer. As shown in Fig. 7, as the impact height and impact number increase, D_p increases but the growth rate decreases, and the D_p growth rate of the sand cushion is the smallest. This is because, as the number of impacts increases, the sand particles around the impact point tend to be denser, and the penetration resistance increases. When the sand particles around the impact point are very dense, the change

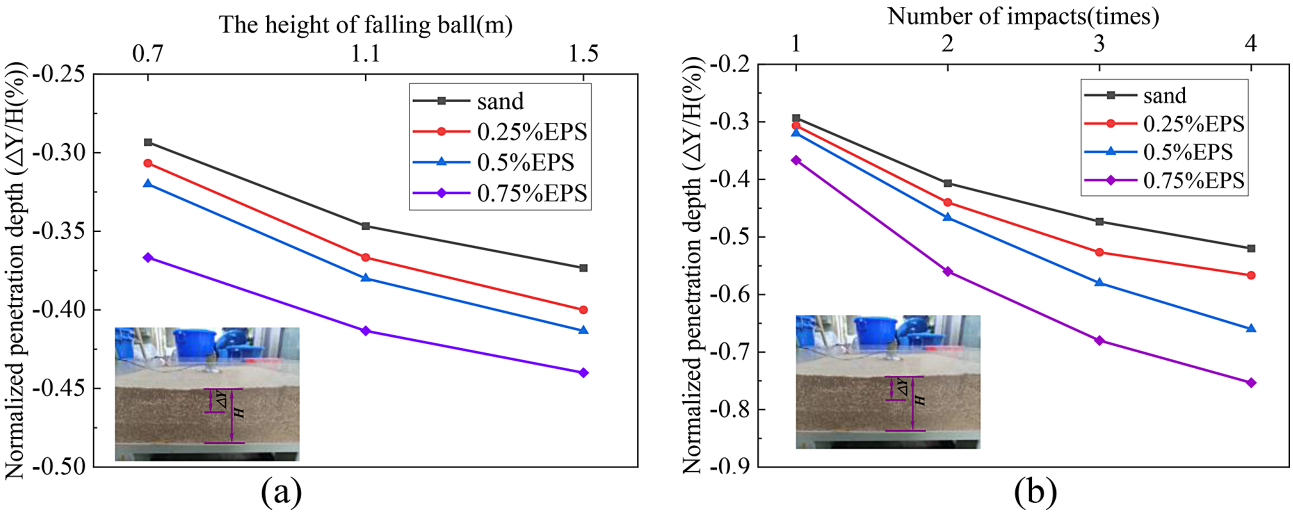

Fig. 7 The response of penetration depth: (**a**) single impact; (**b**) Multiple impacts

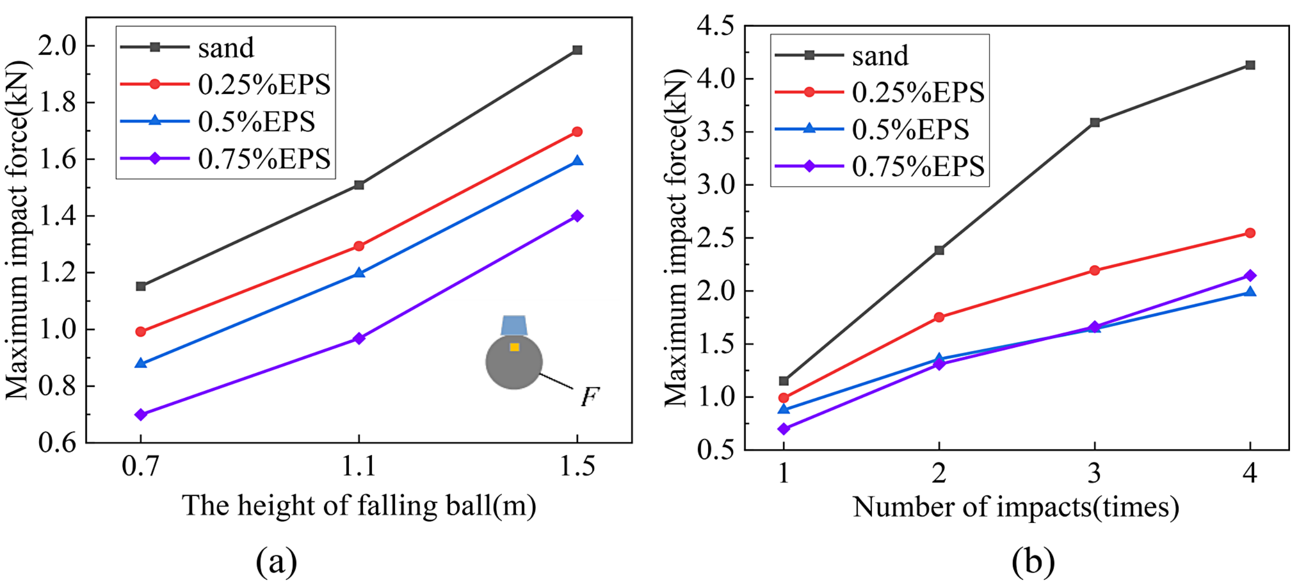

Fig. 8 The response of maximum impact force: (**a**) single impact; (**b**) Multiple impacts

in penetration depth will be very small. Moreover, as the EPS bead content increases, the D_p of the EPS bead-sand cushion increases. When the EPS bead content is 0.75%, the D_p even reaches 75% at the fourth impact. Moreover, EPS beads have great deformation performance and can deform 90% by themselves. Therefore, the D_p of the cushion with higher EPS bead content changes significantly as the impact height and impact number increase.

Maximum impact force

The impact force can be obtained by the formula $F=ma$. As shown in Fig. 8, the maximum impact force (F_{max}) increases with the increase in impact height and impact numbers. The F_{max} of the sand cushion is the largest and changes most significantly. This is because the greater the impact energy and number of impacts, the greater the penetration resistance. Moreover, the F_{max} decreases as the EPS bead content increases under single impacts (Fig. 8a). When the impact height is 1.5 m, the F_{max} values of the cushions with EPS bead content of 0.25%、0.5% and 0.75% are 14.52%, 19.80%, and 29.46% lower than that of the sand cushion respectively. This is due to the high damping and high energy consumption characteristics of EPS beads, which improve the efficiency of the cushion in absorbing impact energy, resulting in an increase in D_p and impact duration time, thereby reducing F_{max}. However, multiple impacts exhibit different patterns. For instance, the F_{max} of the 0.75%EPS cushion is the smallest in the first two impacts but exceeds the 0.5%EPS cushion in the 3rd and 4th impacts (Fig. 8b).

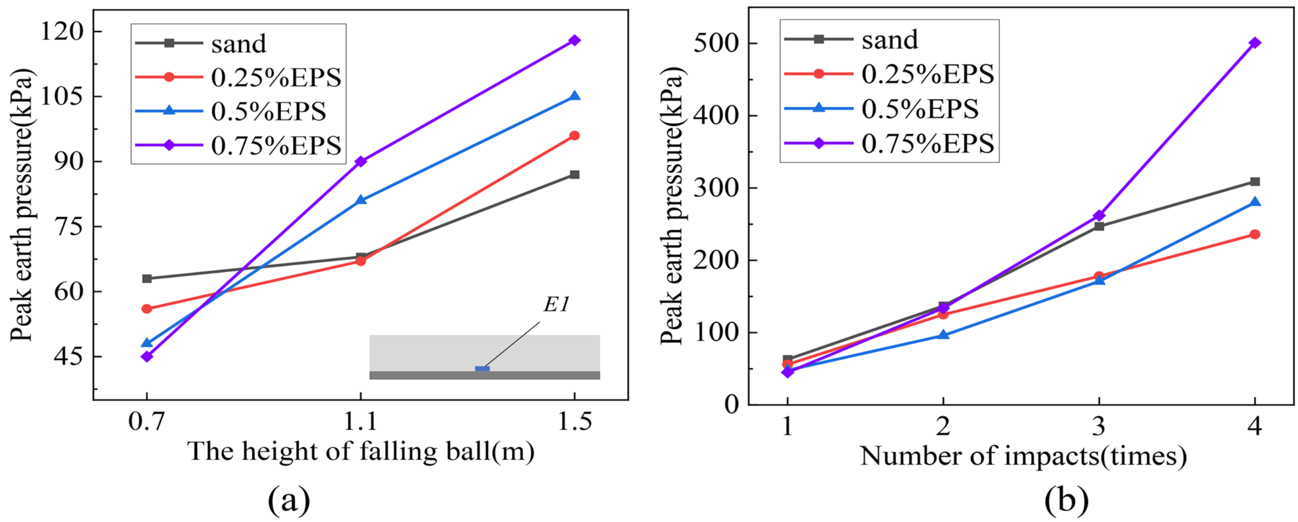

Fig. 9 Impact stress diffusion sketch

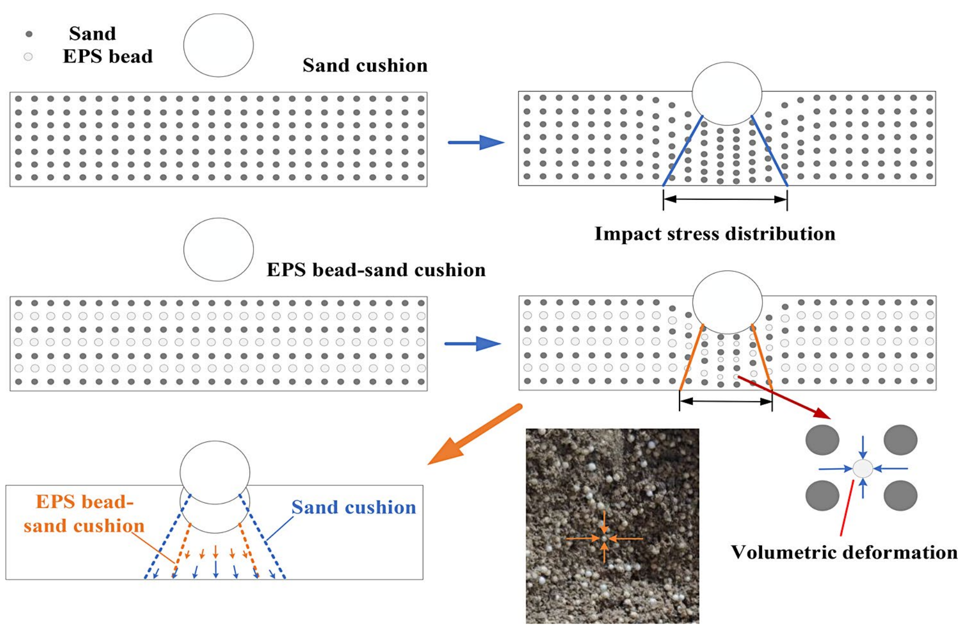

Fig. 10 The response of peak earth pressure: (**a**) single impact; (**b**) Multiple impacts

This is because at the 3rd and 4th impacts, the D_p of the 0.75%EPS cushion has reached 10.2 cm and 11.3 cm respectively, and the retaining thickness of the cushion is less than 1/3, resulting in a significant reduction in buffering effect. Moreover, the buffering capacity of the sand cushion decreases as the sand particles tend to be denser, while the EPS beads can continuously deform themselves to reduce the penetration resistance of the falling ball (Fig. 9), resulting in a smaller F_{max} in the EPS bead-sand cushion.

Peak earth pressure

The impact stress will be transferred to the rock shed through the compression of the buffering material and the friction between the particles. The impact stress is mainly distributed in a conical shape, decreasing in all directions from the impact point. To highlight the variation pattern of earth pressure at the top of the rock shed, the maximum earth pressure $E1_{max}$ at the E1 position of the cushion is discussed, as shown in Fig. 10. As the impact height and the impact number increase, the $E1_{max}$ shows different degrees of increase. When the impact height is 0.7 m, the higher the EPS bead content, the smaller the $E1_{max}$ is. However, as the impact height increases, the $E1_{max}$ of the cushion with higher EPS bead content increases continuously, among which the $E1_{max}$ of the 0.75%EPS cushion is the largest at the impact height of 1.5 m. This is because the D_p of the cushions with higher EPS bead contents is larger at high-impact heights. Although they have a certain reduction effect on the impact force, they have a poor diffusion effect on the impact stress, resulting in earth pressure concentration. Moreover, the $E1_{max}$ exhibits a similar variation pattern under multiple impacts, as shown in Fig. 10b. The 0.75%EPS cushion had the largest $E1_{max}$ at the third impact, and even far exceeds the sand cushion at the fourth impact. It is worth noting that although the $E1_{max}$ at the fourth impact is smaller, the earth pressure growth rate of the 0.5%EPS cushion is much larger than that of the sand cushion. Therefore, under the experimental conditions of this study, the cushion with lower EPS bead content shows better impact stress diffusion under multiple impacts. Furthermore, due to the larger D_p and smaller impact stress diffusion angle, the impact stress of the EPS bead-sand cushions is more concentrated below the impact point and the impact stress distribution is shown in Fig. 9.

Impact stress factor

To better describe the diffusion and attenuation of the impact stress in the cushions, the impact stress factor I is introduced. The projection of the horizontal contact area between the falling ball and the cushion is S ($S = \pi r^2$, r is the radius of the impact crater). Assuming that the maximum impact stress (P_{max}) acting on the cushion is uniformly distributed, P_{max} can be calculated based on the maximum impact force ($P_{max} = F_{max}/S$). Combined with the measured maximum earth pressure $E1_{max}$, the impact stress factor can be obtained by using $I = P_{max}/E1_{max}$. When I>1, it means that the cushion has a better effect on the absorption and diffusion of impact stresses.

Figure 11 shows the change curves of the impact stress factor with the impact height and impact number. The I-value decreases with the increase of the impact height, impact number, and EPS bead content. Moreover, the I-value of the 0.75%EPS cushion is 0.81 at the third impact, meaning that the impact stress diffusion effect almost disappears. That is to say, the cushion with too high EPS bead content has poor impact stress dispersion, and can easily lead to impact stress concentration at high energy or multiple impacts.

Slab vibration

The slab vibrates under the impact of the falling ball, with the most intense vibration occurring at the vertical projection position of the impact point. Figure 12 shows the vibration acceleration response of point A2 of the slab under single impact and multiple impacts. The vibration acceleration amplitude increases as the impact height and impact number increase but decreases as the EPS bead content increases. Furthermore, when the impact height is 1.5 m, the peak acceleration of the 0.75%EPS cushion is only 15.8% of that of the sand cushion. This is due to EPS beads having a high damping ratio, which can absorb part of the vibration energy. It is worth noting that the peak acceleration of the 0.75%EPS cushion exceeds that of the 0.5%EPS cushion at the fourth impact (Fig. 12b). This may be due to the greater D_p of the 0.75% EPS cushion under multiple impacts, resulting in a significant reduction in buffering capacity.

To further study the frequency characteristics of the vibration acceleration, the spectrums of the acceleration

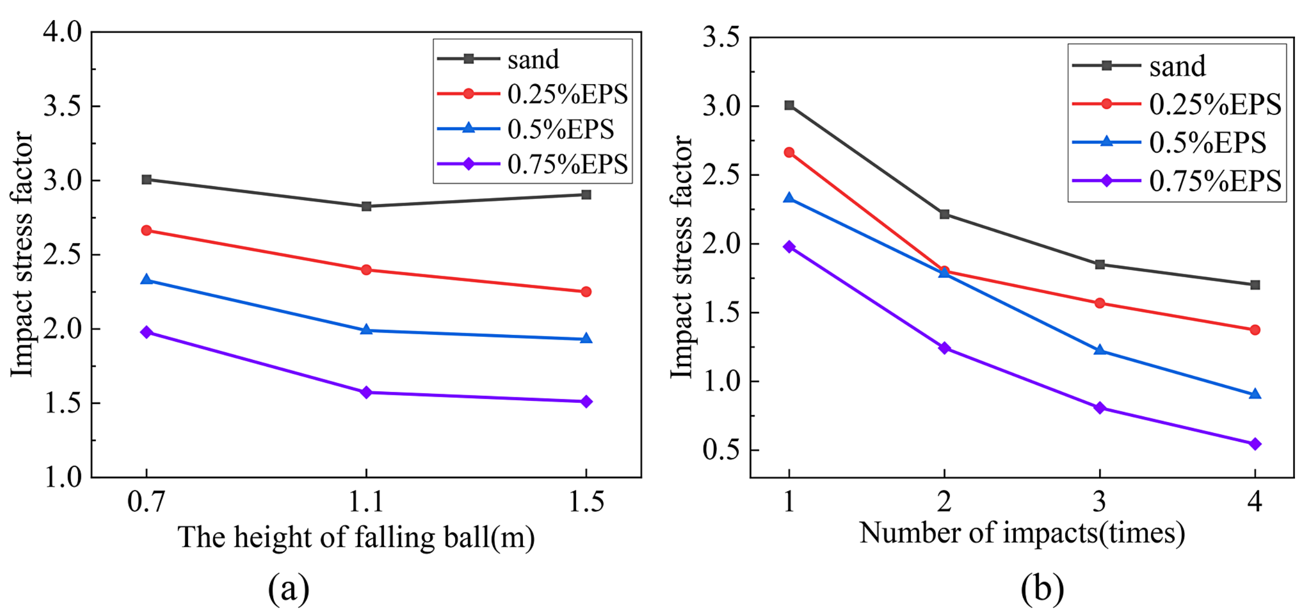

Fig. 11 Impact stress factor: (**a**) single impact; (**b**) multiple impacts

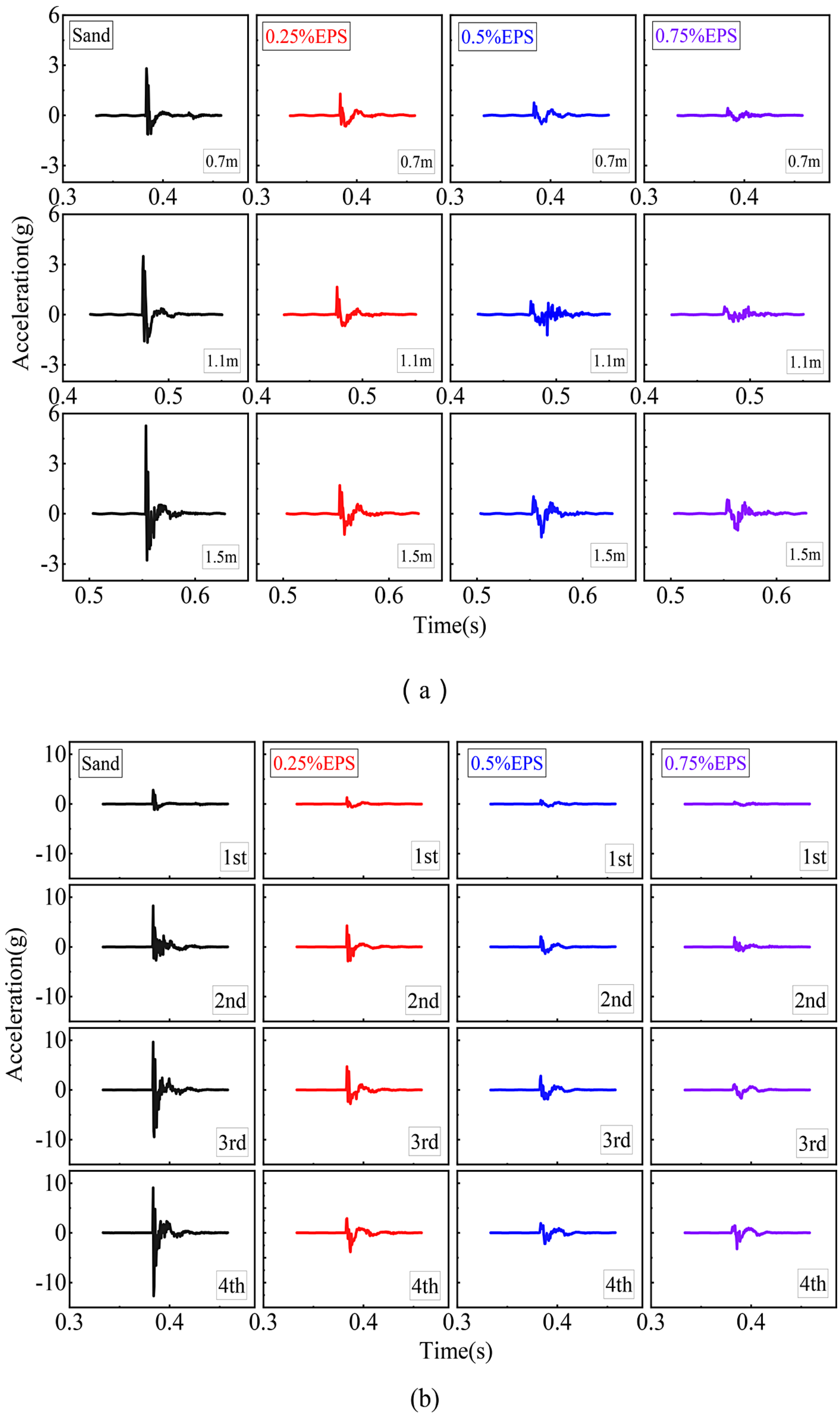

Fig. 12 The response of vibration acceleration: (**a**) single impact; (**b**) multiple impacts

waves were extracted and analyzed using the Fast Fourier Transform (FFT), as shown in Fig. 13. The peak amplitude is distributed at the frequency of 40 to 60 Hz, and the amplitude decreases significantly as the EPS bead content increase, even the peak amplitude of the 0.75%EPS cushion is only 51% of that of the sand cushion at the fourth impact (Fig. 13b). For the single impact (Fig. 13a), there are large amplitude fluctuations at high

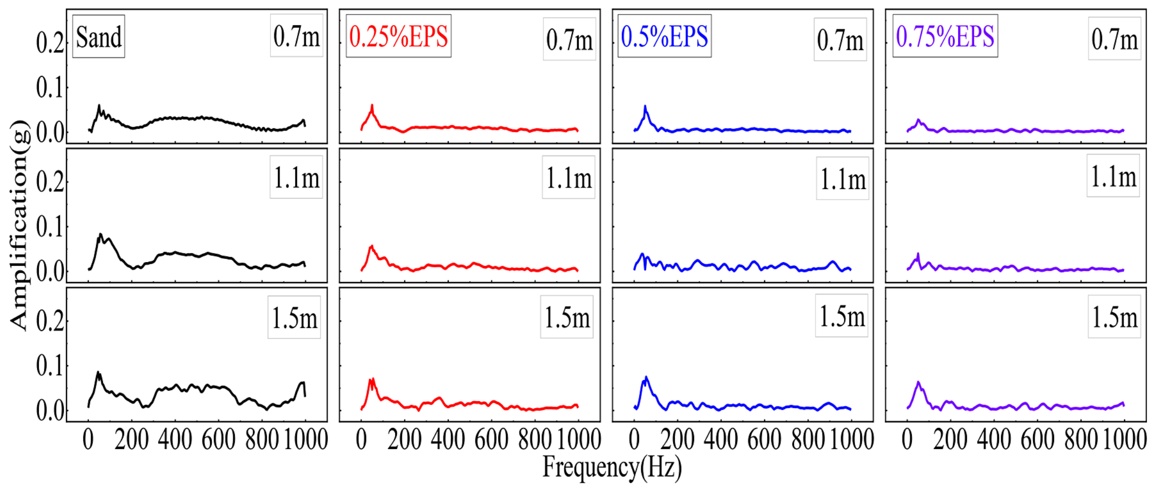

(a)

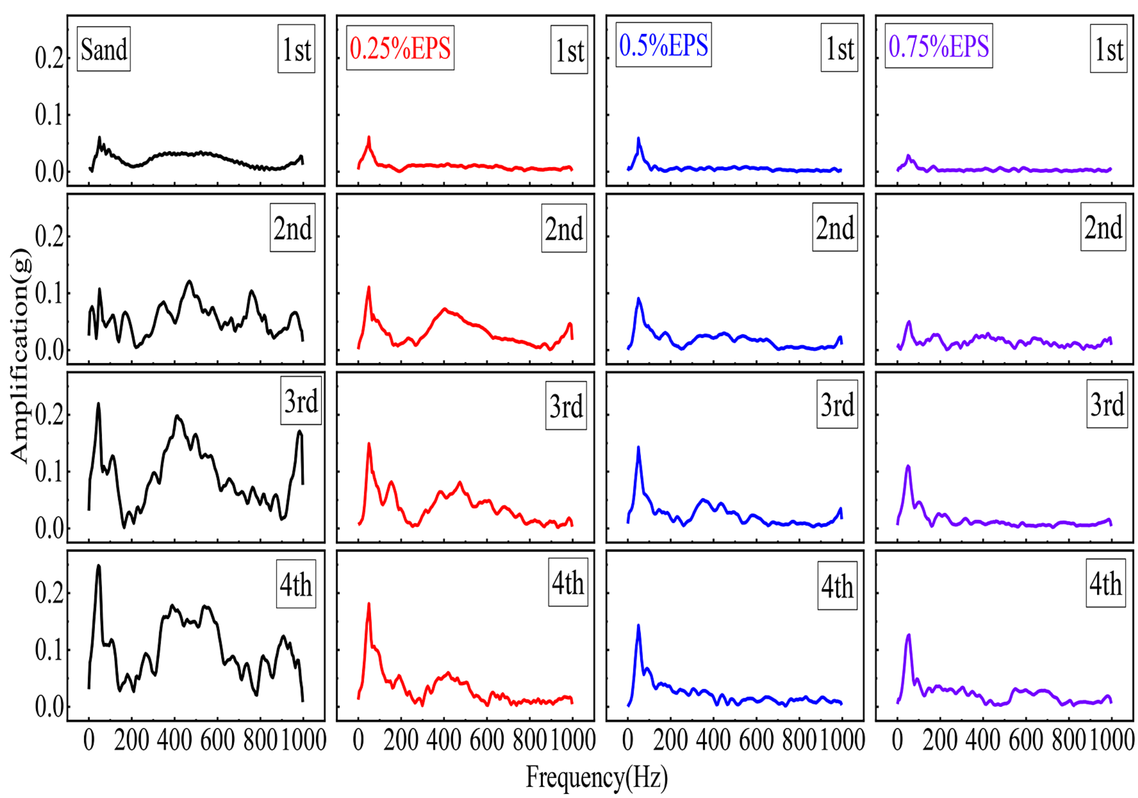

(b)

Fig. 13 Spectral analysis of vibration acceleration: (**a**) single impact; (**b**) multiple impacts

frequencies of sand cushion, while almost no amplitude fluctuations at high frequencies of EPS bead-sand cushions. This may be because the EPS beads increase the damping ratio of the cushions, and the high-frequency vibration waves were absorbed, while the low-frequency vibration waves were greatly weakened. However, the four types of cushions all show varying degrees of amplitude fluctuations in the high-frequency part at the fourth impact (Fig. 13b). This is because the D_p of the cushion is larger at the fourth impact, and the cushion becomes denser, so the remaining cushion thickness is not enough to dissipate high-frequency vibration waves.

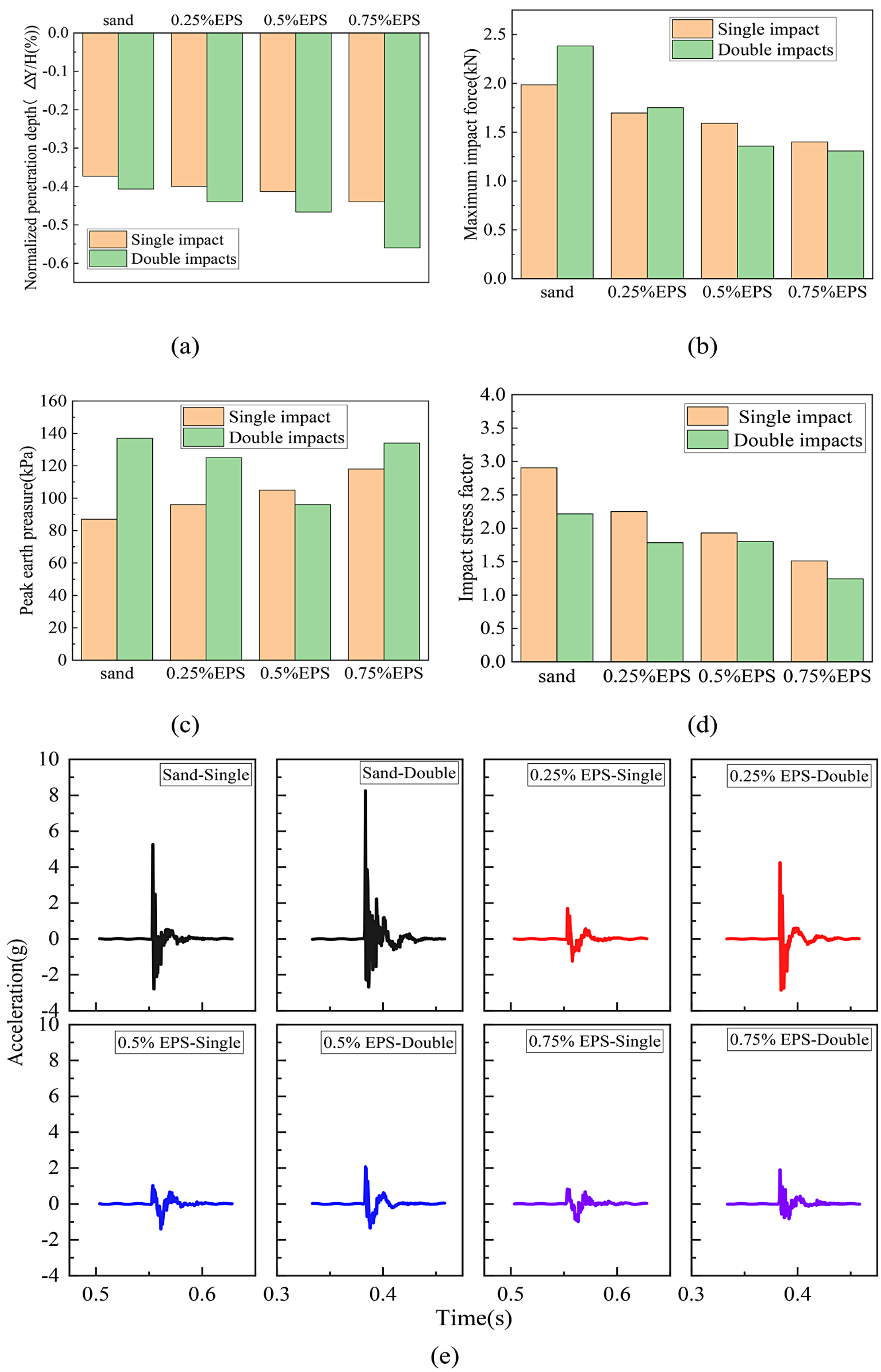

Fig. 14 Comparative analysis of single and multiple impacts: (**a**) depth of penetration; (**b**) maximum impact force; (**c**) peak earth pressure; (**d**) impact stress factor; (**e**) vibration acceleration

Comparative of the single and multiple impacts

Comparative analysis of single impact and multiple impacts can be used to evaluate the buffering mechanism of the cushion under complex working conditions and provide a reference for design and subsequent maintenance. The impact energy of the impact height of 1.5 m is 64.68 J, and the cumulative impact energy of two consecutive impacts at the impact height of 0.7 m (hereinafter referred to as double impacts) is 60.36 J. The impact energies in these two cases are relatively close and can be used for comparative analysis. Figure 14(a) shows the D_p for the single and double impacts. Double impacts produce greater penetration, and the higher the EPS bead content, the greater the D_p. Figure 14(b) shows the F_{max} for the single and double impacts. Although the impact height of the double impacts is only half that of the single impact, the difference in F_{max} is not significant between the two conditions. Furthermore, the F_{max} of the sand cushion and the 0.25%EPS cushion is larger under the double impacts, and the F_{max} is smaller when the EPS bead content is more than 0.5%. This indicates multiple impacts will cause the cushion to become denser and the buffering performance to deteriorate, but high EPS bead content has good deformation coordination properties and can mitigate the degradation of the buffering performance. Figure 14(c) shows the $E1_{max}$ for the single and double impacts. The $E1_{max}$ of 0.5%EPS cushion is smaller under the double impacts, but larger at other cushions. This is because an appropriate amount of EPS beads can improve the performance of the cushion under multiple impacts, but when the EPS bead content is high, the cushion is easily penetrated or the remaining thickness becomes thinner, resulting in poor impact stress diffusion. The impact stress factor under the single and double impacts is shown in Fig. 14(d). The *I*-value under the double impacts is smaller than the single impact. This illustrates that the cumulative effect from multiple impacts can easily lead to poor impact stress absorption and diffusion. In addition, Fig. 14(e) shows the vibration acceleration under the single and the second impact of double impacts. Although the second impact had less impact energy, the vibration acceleration amplitude is greater than that of the single impact. This is also due to the cumulative effect of multiple impacts. Therefore, the cumulative effect of multiple impacts will lead to a significant decrease in the buffering performance of the cushion. It is necessary to monitor the buffering condition of the cushion during actual projects and to maintain it as necessary.

F_{max} estimation of EPS bead-sand cushions

Most of the existing F_{max} estimation methods are based on spherical rockfall and sand cushion, and the F_{max} of sand cushion under single impact is usually calculated

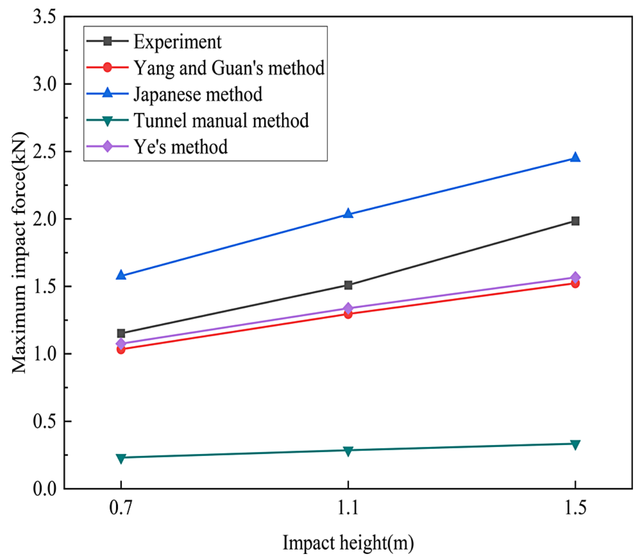

Fig. 15 Comparison of experimental and theoretical calculations results on maximum impact force of single impact on sand cushion

according to Yang Qixin and Guan Shubao method, Japanese method, Tunnel Manual method, and Ye Siqiao method (Xu 2016). Figure 15 shows the comparison of experimental and theoretical results on the maximum impact force of single impacts on the sand cushion. The experimental results are located between the Japanese method and Ye's method. To further promote the use of EPS bead-sand cushions, a method for calculating the F_{max} of EPS bead-sand cushions is proposed based on the sand cushion. It can be seen from Fig. 11(a) that the change patterns of F_{max} with impact height for the cushions with different EPS bead contents are relatively similar, which can be obtained by discounting the F_{max} of the sand cushion using formula (3.1). The discounted F_{max} of the sand cushion was fitted to the EPS bead-sand cushions using the least squares method, and the

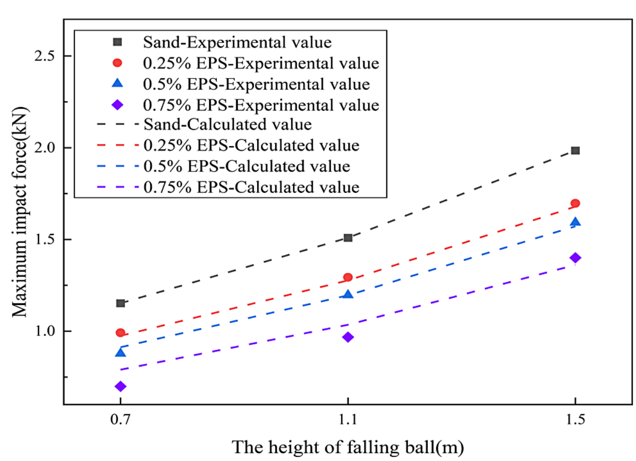

Fig. 16 Comparison of experimental and theoretical calculations results of the maximum impact force of the cushions with different EPS bead contents under single impact

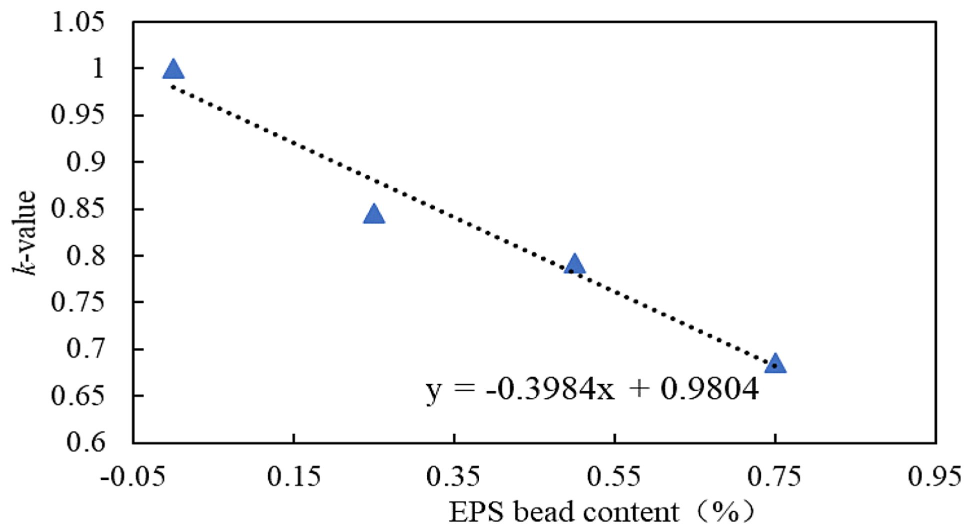

Fig. 17 The relationship between *k* value and EPS bead content

discount factor *k* of the 0.25%, 0.5%, and 0.75% EPS cushions was obtained to be 0.846, 0.792, and 0.686, respectively. The calculated F_{max} is consistent with the EPS bead-sand cushion, as shown in Fig. 16, which can better reflect the F_{max} of the cushions with different EPS bead contents. To facilitate the promotion and application of EPS bead-sand cushions in engineering, the relationship curve between *k*-value and EPS bead content was plotted, as shown in Fig. 17. The *k* value changes with the bead content close to a linear law, and its expression can be expressed as Eq. (3.2).

$$F_{EPS} = kF_{sand} \tag{3.1}$$

$$k = -0.3984C + 0.9804 \tag{3.2}$$

where F_{EPS} is the maximum impact force of EPS bead-sand cushion; *k* is the discount factor; F_{Sand} is the maximum impact force of sand cushion; and *C* is the EPS bead content.

Conclusions

EPS bead-sand cushion has great potential in rockfall protection, but its buffering mechanism is not yet clear. In this study, a series of impact tests were carried out to investigate the buffering characteristics of EPS bead-sand cushions, and the buffering performance of the cushions with different EPS bead contents under single impact and multiple impacts were comparatively analyzed. The main conclusions are as follows:

(1) EPS beads can reduce the stiffness of the sand cushion and increase impact duration time. Under low-energy impact, the maximum impact force, impact stress, and slab vibration acceleration were significantly reduced when EPS beads were mixed in the sand cushion.

(2) The cushions with high EPS bead content have excellent buffering properties, but are easily penetrated by high-energy impact or multiple impacts, resulting in excessive concentration of impact stress. Therefore, the EPS bead content cannot be too high, especially in the areas that are often subject to high-energy impact or multiple impacts.

(3) Under the same total impact energy, double low-energy impacts produce greater penetration than a single high-energy impact. The cumulative effect of multiple impacts significantly reduces the buffering performance of the EPS bead-sand cushions. In actual projects, the buffering condition of the cushion should be monitored for maintenance.

(4) A simple estimation method for calculating the maximum impact force of the EPS bead-sand cushion was proposed based on the sand cushion estimation methods, which is helpful in promoting the use of the EPS bead-sand cushion.

Acknowledgements
This study was supported by Shanghai Pujiang Programme (23PJD101), the National Natural Science Foundation of China (41877224), the Fundamental Research Funds for the Central Universities, and the China Scholarship Council (202006265003).

Author contributions
Feifan Ren and Jiahao Liu: Data analysis and Writing.Feifan Ren, Jiahao Liu and Qiangqiang Huang: Formal analysis.Jiahao Liu, Huan Ding and Zhipeng Hu: Experiment.Guan Wang and Feifan Ren: Methodology.

Data availability
No datasets were generated or analysed during the current study.

Declarations

Competing interests
The authors declare no competing interests.

Received: 31 May 2024 / Accepted: 2 October 2024
Published online: 14 October 2024

References
Alaie R, Chenari RJ (2018) Cyclic and post-cyclic shear behaviour of interface between Geogrid and EPS beads-sand backfill. KSCE J Civ Eng 22(9):3340–3357. https://doi.org/10.1007/s12205-018-0945-2

Alaie R, Jamshidi CR (2019) Dynamic properties of EPS-Sand mixtures using cyclic Triaxial and Bender element tests. Geosynth Int 26(6): 63-579. https://doi.org/10.1680/jgein.19.00034

Alaie R, Chenari J, R., Karimpour-Fard M (2021) Shaking table study on Sand-EPS beads-mixtures using a Laminar Box. Geosynth Int 28(3): 224–237. https://doi.org/10.1680/jgein.20.00039

Bhatti AQ (2015) Falling-weight impact response for prototype RC type rock-shed with sand cushion. Mater Struct 48(10):3367–3375. https://doi.org/10.1617/s11527-014-0405-5

Cai X, Li S, Xu H et al (2021) Shaking table study on the seismic performance of geogrid reinforced soil retaining walls[J]. Advances in Civil Engineering, 2021: 1–16. https://doi.org/10.1155/2021/6668713

National Bureau of Statistics of China (2023) China Statistical Yearbook 2023. Geological disasters and prevention and control [EB/OL]. https://www.stats.gov.cn/sj/ndsj/2023/indexch.htm

Deng A, Xiao Y (2010) Measuring and modeling proportion-dependent stress-strain behavior of EPS-Sand mixture. Int J Geomech 10(6):214–222. https://doi.org/10.1061/(ASCE)GM.1943-5622.0000062

Di Prisco C, Vecchiotti M (2010) Design charts for evaluating Impact forces on Dissipative Granular Soil cushions. J Geotech GeoEnviron Eng 136(11):1529–1541. https://doi.org/10.1061/(ASCE)GT.1943-5606.0000363

Dorren LK, A (2003) A review of rockfall mechanics and modelling approaches. Prog Phys Geogr 27(1):69–87. https://doi.org/10.1191/0309133303pp359ra

Ertugrul OL, Kiwanuka A (2023) Dynamic analysis of rock fall impact for a cantilever rock shed with geofoam cushion[J]. Eur J Environ Civil Eng 27(5):1989–2014. https://doi.org/10.1080/19648189.2022.2107577

Ge Q, Zuo W, Liu R et al (2022) Experimental studies for shear and multi-impact resistance performance of sand–geofoam material[J]. Buildings 12(5):633. https://doi.org/10.3390/buildings12050633

He SM, Wang DP, Wu Y et al (2014) Mechanical mechanism and prevention technology of avalanche rolling rock disaster[J]. Nat Magazine 36(5):336–345. https://doi.org/10.3969/j.issn.0253-9608.2014.05.004

Hou TS, Yang KX (2021) Experimental study on static soil pressure characteristics of EPS particle mixed lightweight soil filler behind retaining walls [J] geotechnical mechanics. 42(12):3249–3259. https://doi.org/10.16285/j.rsm.2020.1598

Hsu SH, Maegawa K, Chen LH (2016) Experimental study on the EPS-based shock absorber for rock-shed[J]. GEOMATE J 11(26):2534–2540

Hsu SH, Maegawa K, Hama A (2018) Full-scale testing and modeling of rock-shed shock absorbers under impact loads[J]. Int J Protective Struct 9(2):157–173. https://doi.org/10.1177/2041419617728

Kawahara S, Muro T (2006) Effects of dry density and thickness of sandy soil on impact response due to rockfall[J]. J Terrramech 43(3):329–340. https://doi.org/10.1016/j.jterra.2005.05.009

Khajeh A, Jamshidi Chenari R, Payan M (2020) A review of the studies on soil-EPS composites: beads and blocks[J]. Geotech Geol Eng 38:3363–3383. https://doi.org/10.1007/s10706-020-01252-2

Khajeh A, Ebrahimi SA, MolaAbasi H et al (2021) Effect of EPS beads in lightening a typical zeolite and cement-treated sand[J]. Bull Eng Geol Environ 80(11):8615–8632. https://doi.org/10.1007/s10064-021-02458-1

Liu C, Yu Z, Zhao S (2020) Quantifying the impact of a debris avalanche against a flexible barrier by coupled DEM-FEM analyses[J]. Landslides 17:33–47. https://doi.org/10.1007/s10346-019-01267-8

Luo J, Xiao JC, Ma KJ et al (2019) Research on buffering performance of multiple types of soil under rockfall impact[J]. J Disaster Prev Mitigation Eng 39(01):164–. https://doi.org/10.13409/j.cnki.jdpme.2019.01.023

Meng X, Jiang Q, Han J et al (2022) Experimental investigation of geogrid-reinforced sand cushions for rock sheds against rockfall impact[J]. Transp Geotechnics 33:100717. https://doi.org/10.1016/j.trgeo.2022.100717

Ren F, Huang Q, Wang G (2020) Shaking table tests on reinforced soil retaining walls subjected to the combined effects of rainfall and earthquakes[J]. Eng Geol 267:105475. https://doi.org/10.1016/j.enggeo.2020.105475

Shen W, Zhao T, Dai F (2021) Influence of particle size on the buffering efficiency of soil cushion layer against rockfall impact[J]. Nat Hazards 108:1469–1488. https://doi.org/10.1007/s11069-021-04741-6

Wang X, Xia Y, Zhou T (2018) Theoretical analysis of rockfall impacts on the soil cushion layer of protective structures[J]. Adv Civil Eng 2018:1–18. https://doi.org/10.1155/2018/9324956

Wang X, Zhou TY, Shi JT et al (2019) Theoretical and LS-DYNA simulation study of free-fall based rockfall impact on soil layer[J]. J Beijing Jiaotong Univ 43(4):9–17. https://doi.org/10.11860/j.issn.1673-0291.20190015

Wang SZ, Xiaojun JB et al (2016) Numerical analysis of dynamic response and impact resistance study of tunnel large-span shed hole under rockfall impact. Explosion and Shock, 36(04):548 ~ 556. DOI: 1011883 /1001–1455(2016) 04-0548-09

Wei LW, Chen H, Lee CF et al (2014) The mechanism of rockfall disaster: a case study from Badouzih, Keelung, in northern Taiwan[J]. Eng Geol 183:116–126. https://doi.org/10.1016/j.enggeo.2014.10.008

Xu S (2016) Research on the calculation method of falling rock impact force [D]. Master's thesis. Chongqing: Chongqing Jiaotong University

Yan S, Wang Y, Wang D et al (2022) Application of EPS geofoam in rockfall galleries: insights from large-scale experiments and FDEM simulations[J]. Geotext Geomembr 50(4):677–693. https://doi.org/10.1016/j.geotexmem.2022.03.009

Yao CY (2018) Diffusion mechanism of falling rock impact force [D]. Chongqing Jiaotong University

Yu ZX, Zhao L, Guo LP et al (2019) Full-scale impact test and numerical simulation of a new-type resilient rock-shed flexible buffer structure[J]. Shock and Vibration, 2019. https://doi.org/10.1155/2019/7934696

Žabota B, Kobal M (2020) A new methodology for mapping past rockfall events: from mobile crowdsourcing to rockfall simulation validation[J]. ISPRS Int J geo-information 9(9):514. https://doi.org/10.3390/ijgi9090514

Zhang Y, Xie L, He B et al (2022) Research on the Impact Force of Rockfall Impacting Sand cushions with different Shapes[J]. Appl Sci 12(7):3540. https://doi.org/10.3390/app12073540

Zhao P, Xie L, Li L et al (2018a) Large-scale rockfall impact experiments on a RC rock-shed with a newly proposed cushion layer composed of sand and EPE[J]. Eng Struct 175:386–398. https://doi.org/10.1016/j.engstruct.2018.08.046

Zhao P, Xie L, He B et al (2018b) Experimental study of rock-sheds constructed with PE fibres and composite cushion against rockfall impacts[J]. Eng Struct 177:175–189. https://doi.org/10.1016/j.engstruct.2018.09.073

Zhao P, Yuan S, Li L et al (2021) Experimental study on the multi-impact resistance of a composite cushion composed of sand and geofoam[J]. Geotext Geomembr 49(1):45–56. https://doi.org/10.1016/j.geotexmem.2020.09.004

Zhao P, Liu J, Zhang Y (2023) Experimental and numerical investigations on buffer performance of geofoam subjected by the impact of falling rocks with respect to different shapes[J]. Geotext Geomembr 51(4):108–124. https://doi.org/10.1016/j.geotexmem.2023.04.006

Publisher's note